

FIELD TESTING OF HIGHWAY SIGN SUPPORT STRUCTURES

By Kipp A. Martin,¹ Mohammad R. Ehsani,² A. M. ASCE,
and Reidar Bjorhovde,³ F. ASCE

ABSTRACT: The results of field tests for two monotube highway sign support structures with spans of 60 and 100 ft are presented. The intent of the study was to compare field measurements with previously conducted analytical results, including the possibility of resonance due to vortex shedding. Wind speeds of up to 23.2 mph were recorded during the tests. Although the analytical studies predicted resonance tendencies at several lower wind speeds, this did not take place during the field tests due to the inherent damping of the structures. Measured stresses were analyzed statistically to account for the cyclic nature of the loads, to assure a high level of confidence in the maximum stress levels. There was good correlation between computed and measured stresses, all of which were found to be well below allowable values. The adequacy of previous design recommendations was verified.

INTRODUCTION

As the width of highways has grown, so have the sizes of the necessary sign support structures, until today spans in excess of 100 ft are not uncommon. To support signs over these large spans, truss-type structures have traditionally been used. These typically consist of two columns supporting a truss or trichord element, and the traffic signs are arranged in the desired locations and bolted in place.

The design of sign support structures is based on the American Association of State Highway and Transportation Officials's (AASHTO) 1975 "Standard Specifications for Structural Supports for Highway Signs, Luminaries and Traffic Signals." For convenience, this document will be referred to in the following as the Specifications.

The Specifications set minimum performance guidelines. Among these are criteria governing deflections. Essentially, the maximum static dead load deflection, in units of feet, is limited to the empirical value of $d^2/400$, where d = the depth of the sign in feet. The rationale and consequences of this approach have been discussed by Ehsani and Bjorhovde (1986).

Over the years, the performance of the truss structures has generally been satisfactory. However, there are some drawbacks to their use. They are expensive to fabricate, and for that reason are not as economical as some of the pre-engineered structures that are available. One of the latter types that has seen increased use is the monotube sign support structure, which is significantly lighter as well as more attractive than most truss structures.

¹Struct. Engr., Cannon and Assoc., 406 S. 4th Avenue, Tucson, AZ; formerly Grad. Student, Univ. of Arizona, Tucson, AZ 85721.

²Asst. Prof. of Civ. Engrg. and Engrg. Mech., Univ. of Arizona, Tucson, AZ.

³Prof. of Civ. Engrg. and Engrg. Mech., Univ. of Arizona, Tucson, AZ.

Note.—Discussion open until September 1, 1987. To extend the closing date one month, a written request must be filed with the ASCE Manager of Journals. The manuscript for this paper was submitted for review and possible publication on July 17, 1986. This paper is part of the *Journal of Structural Engineering*, Vol. 113, No. 4, April, 1987. ©ASCE, ISSN 0733-9445/87/0004-0850/\$01.00. Paper No. 21443.



FIG. 1.—60-ft Monotube Structure Located in Tucson, Arizona



FIG. 2.—100-ft Monotube Structure Located in Phoenix, Arizona

Monotube structures are constructed of linearly tapering elements that have a constant wall thickness. The columns are one-piece tapered members with the largest diameter at the base. The beam normally consists of two tapered pieces that are joined with the largest diameter at midspan. Beams of longer spans may consist of three pieces, with the middle one having a constant diameter. Figs. 1 and 2 show the structures that were tested as part of this study.

Unfortunately, the Specifications do not provide much information on the design of monotube structures. The absence of adequate design guidelines can be partly attributed to the sparsity of research and engineering data on the strength and behavior of such structures. The first major work in this area was a project conducted by Ehsani, et al. (1985) in 1984 at the University of Arizona. It was found that the $d^2/400$ deflection criterion as inappropriate for monotube structures. Dead load deflections in excess of the $d^2/400$ limit were calculated, although the stresses associated with these deflections were well below the allowable levels.

The first monotube study was purely analytical and the accuracy of the results obtained is a function of the assumptions that were made to

model the structure. It is important to compare such theoretical results with actual performance data for a real structure to verify the modeling, as well as the responses that have been found. The latter should be obtained from testing, preferably using a full-scale structure being subjected to a variety of service conditions. With such test data and correlations in hand, improved design guidelines can be developed.

SCOPE

Before the validity of any analytical study can be fully accepted, its results should be compared to the actual behavior of the subject in question. While the study by Ehsani, et al. (1985), provided detailed data on the behavior of monotube structures, it lacked comparison with the performance of an actual structure.

The study presented here was conducted in three parts. In the first, two actual structures were modeled for computer analysis. Part two involved field testing of the same two structures. By testing the structures under service conditions, the true response was obtained. The final part of the study was aimed at comparing and evaluating the results obtained in the first two parts. Through this comparison, it was possible to judge the validity of the computer model, as well as to determine whether problem conditions such as resonance were developing. Details of the analytical and experimental work that is reported in the following are given by Martin, et al. (1985).

STRUCTURAL RESPONSE UNDER WIND LOADS

For most sign structures, the only loads acting on the structure are gravity and wind. The forces due to gravity are simply the self-weight of the structure as well as the weight of the ice that may attach to the structure during certain times of the year in many geographical areas. The magnitude and effect of these loads on the structure are relatively easy to determine.

In contrast to the gravity loads, which are static, wind loads are dynamic. The wind blowing on a monotube structure acts primarily in two ways. The first is drag on the signs and tubes of the structure, which is a static force. Due to the low coefficient of drag for cylindrical objects, the drag on the tubular elements of a monotube structure is negligible. An approximation of the drag on the signs is incorporated in the computation of the static equivalent of the wind forces in the direction perpendicular to the plane of the structure.

The second action of the wind is a phenomenon known as vortex shedding. Air flowing around an object will develop vortices in the wake which will alternate from one side of the object to the other. These alternating vortices cause the object to vibrate in the plane perpendicular to the direction of the wind.

The magnitude of the vortex forces depends on three major factors, namely the wind velocity, the diameter of the tubular elements of the structure, and the viscosity of the air. While vortex shedding may occur for all values of the Reynolds Number R a deterministic solution can be obtained in the range of $300 < R < 3 \times 10^5$ only. The frequency of the

shedding is a function the Strouhal Number, S , which in turn is related to the Reynolds Number (Fung 1955; Hoerner 1965).

To account for the random force amplitude, Weaver (1961) experimentally determined that root-mean square (rms) values of the force coefficient, C_L , denoted as \bar{C}_L , and obtained an expression for the vortex shedding forces as

$$F(t) = \frac{1}{2} \rho V^2 A_p \bar{C}_L \sin \Omega t \dots \dots \dots (1)$$

where ρ = density of dry air; V = wind velocity; A_p = projected area of the cylinder; Ω = frequency of the vortex shedding; and t = time.

The determination of Ω is critical in the use of this equation, and can be determined from the equation (Fung 1955):

$$\Omega = \frac{SV}{D} \dots \dots \dots (2)$$

where S = Strouhal number; and D = the cylinder diameter. For a complete derivation of the vortex shedding force (see Ehsani, et al. 1985).

ANALYSIS OF MONOTUBE STRUCTURES

To help in developing the design guidelines, as well as to provide data for a detailed comparison with the results of full-scale testing, extensive structural analyses were performed on the two structures that had been selected for the field testing. The response of the models under static and dynamic loading was determined, including details on stresses and deflections.

For this study, the Arizona Department of Transportation provided shop drawings and site plans for two sign structures. Both of these had been designed in accordance with the AASHTO Specifications (1975). The structures had spans of 60 and 100 ft as shown in Figs. 1 and 2. Detailed dimensions are shown in Figs. 3 and 4. It is noted that the 100-ft structure used a three-segment beam where the center segment had a constant diameter. The longer span structure was located at University Drive and Hohokam Expressway in Phoenix, Arizona; at the time, apart from the freeways, the surrounding area was undeveloped. The shorter span structure was located across North Oracle Road at Miracle Mile in Tucson, Arizona; the surrounding area consisted primarily of one- and two-story residential and commercial buildings.

The beam-to-column connection provides some moment resistance to vertical loads and essentially free rotation under horizontal loads. A more detailed discussion of the connection is given in by Ehsani, et al. (1985). The details of the column base are such that it can reasonably be assumed to be fixed.

For each structure, a finite element model was developed following generally accepted guidelines. The elements in both structures were modeled as beam elements with three translational and three rotational degrees of freedom at each node. Hollow circular sections were used for the beam and column elements, while an I-shape was used for the beam-to-column connection elements. It was not possible to model the struc-

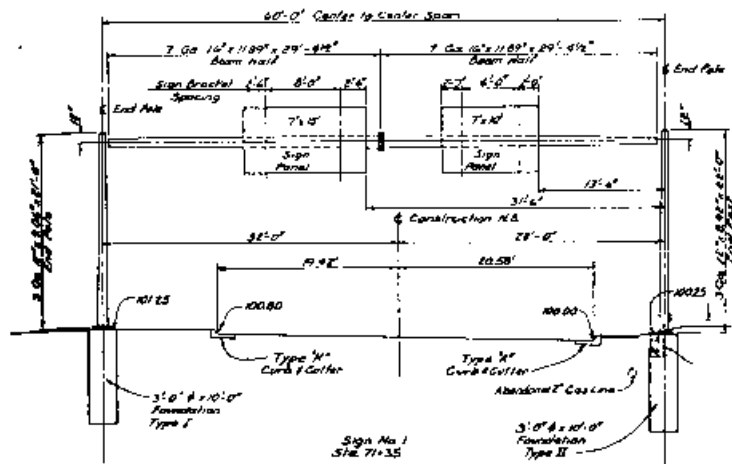


FIG. 3.—Dimensions of 60-ft Structure

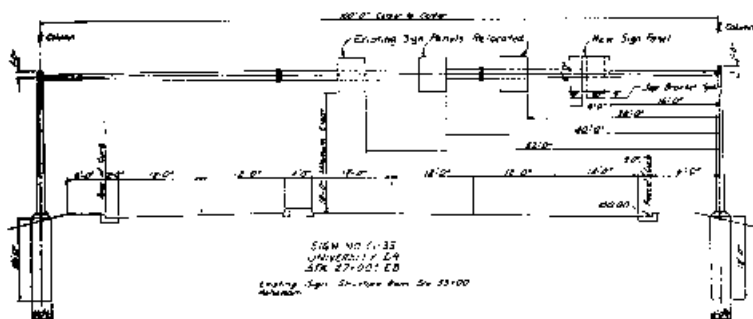


FIG. 4.—Dimensions of 100-ft Structure

tures exactly as they appear in the field because the finite element program used can only handle prismatic members. To circumvent this limitation, each element was assumed to have a constant cross section, with dimensions equal to the average of the two end cross sections of the element in the actual structure. The wall thickness of the circular elements was taken as the minimum specified by the shop drawings.

The shear capacity of a connection is based on its cross-sectional area, while the flexural capacity depends on the moment of inertia. To ensure a realistic behavior for shear, the connection was modeled as a short I-section beam with the same area as the actual connection. The weak axis of the I-beam was oriented to give the least bending resistance in the horizontal direction, reflecting the simple support condition for the beam under the action of horizontal (perpendicular to the plane of the mono-tube structure) loads. The element was proportioned to give a moment capacity in the vertical direction approximating that of the real connection. The I-section was actually similar to a flat plate, as the flanges were

TABLE 1.—Natural Frequencies for 60-ft and 100-ft Structures

Mode (1)	60-ft Structure		100-ft Structure	
	2D, cps (2)	3D, cps (3)	2D, cps (4)	3D, cps (5)
1	2.834	2.295	1.467	1.467
2	3.265	2.834	3.055	1.479
3	12.290	3.265	5.001	3.055
4	27.301	4.293	10.872	3.868
5	31.760	7.925	19.263	5.001
6	39.714	12.290	19.481	6.193
7	47.312	16.646	36.418	9.118
8	74.169	27.301	37.518	10.872
9	92.693	29.307	42.252	13.874
10	102.730	31.934	56.589	19.263

only slightly wider than the web and of negligible thickness (1×10^{-20} in.).

In selecting the nodal points for each structure, a node was placed at the actual attachment points of each traffic sign, for signs wider than four ft, and at the center of the sign for signs four ft wide or less. In this manner, the mass of the signs would be applied at a node. A node was also placed at the midspan of the beam to be able to determine deflections and stresses at this point.

All loads were applied to the models as nodal loads. The magnitudes of these loads were computed as discussed previously. Each structure was analyzed for various combinations of static and dynamic loads for wind speeds between 2.5 mph and 20.0 mph, in increments of 2.5 mph. Additional runs were made for 22.5 mph and 23.2 mph for the 60 ft structure and 21.3 mph for the 100 ft structure. Above the largest wind speed for each structure, the vortex shedding becomes random, and the analytical solution is no longer applicable (Ehsani and Bjorhovde 1986).

In addition to the static and dynamic load analysis, the first ten two-dimensional (2D) and three-dimensional (3D) natural frequencies were also determined, assuming zero damping. These are given in Table 1.

Analytical Results.—For the wind speeds considered, the gravity loads due to the weight of the structure govern in all cases. The stresses at midspan are principally due to the weight of the structure. The magnitudes of the in-plane bending stresses are independent of the wind speed. For the 60-ft structure, the maximum stress was 5.11 ksi, which is about 15% of the yield stress of 34 ksi. The magnitude of the maximum stress for the 100-ft structure was 10.92 ksi, which is about 32% of the yield stress. The maximum normal stress at the column base for the 60-ft structure was 2.64 ksi, and for the 100-ft structure it was 3.25 ksi.

At the connection between the column and the beam, shear stress is the governing factor. For both structures, the finite element model showed some normal stress, but this is largely due to the way the joint was modeled rather than any actual stress. The shear stress at the joint was close to constant for both structures, and the gravity loads appear to

govern. For the 60-ft structure, the maximum shear stress was 2.64 ksi, and for the 100-ft structure, it was 4.53 ksi. Both are well below the shear yield stress of the steel, which is 19.4 ksi.

As has been seen, the stresses at the three critical locations on each structure are significantly below the representative yield values of the steel. However, neither structure was able to meet the $d^2/400$ deflection criterion. For the 60-ft structure, which has a sign depth of seven ft, the maximum allowable deflection according to Specifications (AASHTO 1975) is: $d^2/400 = 7^2/400 = 0.123$ ft = 1.48 in. For the 100-ft structure with a sign depth of 5 ft, the allowable deflection is: $d^2/400 = 5^2/400 = 0.076$ ft = 0.75 in.

These compare to the computed deflections of 1.12 and 5.51 in. for the 60- and 100-ft structures, respectively. Since the stresses are very low in both cases, this illustrates why the $d^2/400$ deflection criterion is unrealistic for monotube structures.

FIELD TESTING OF FULL-SCALE STRUCTURES

The second phase of the study consisted of the testing of actual sign support structures under service conditions. This was accomplished by instrumenting the Phoenix and Tucson structures with electrical resistance strain gages, as well as an anemometer to determine wind velocity and direction. The data were used to determine the stresses and strains at a number of important locations in the structures, and subsequently to evaluate the correlation between theoretical and actual structural performance. The data collection for the Tucson structure was carried out during the months of February–April, and for the Phoenix structure during the months of May–July. Due to the high ambient temperatures in central and southern Arizona during the summer months, it was necessary to calibrate the instruments and the strain gage readings to eliminate the effects of high temperatures.

Experimental Results.—The portable data collection equipment was capable of reading the anemometer and strain gages approximately every 34 sec (Martin, et al. 1985). The data acquisition unit first read and stored the wind speed and direction. Using these values, the magnitude of the wind component perpendicular to the plane of the structure was then computed and stored. It is noted that while the gage readings were accomplished quickly, most of the time that was needed was used to retrieve and store the data.

Due to the vibrating nature of the structures, the strain gage readings were not necessarily always made at peaks. The readings might have been taken at any point in the cycle, and it was therefore determined that a statistical evaluation of the data was the only way in which logical explanations of the results could be provided.

The analysis was conducted for each gage for all wind speeds using increments of 1 mph. Each nominal wind speed covered a range of 0.5 mph on either side of the nominal value. Therefore, actual wind speed values exactly halfway between two nominal wind speed increments were rounded up to the higher value.

For the 60-ft structure, a total of 1,244 readings were made by each gage. For the 100-ft structure, 1,133 readings were taken per gage. For

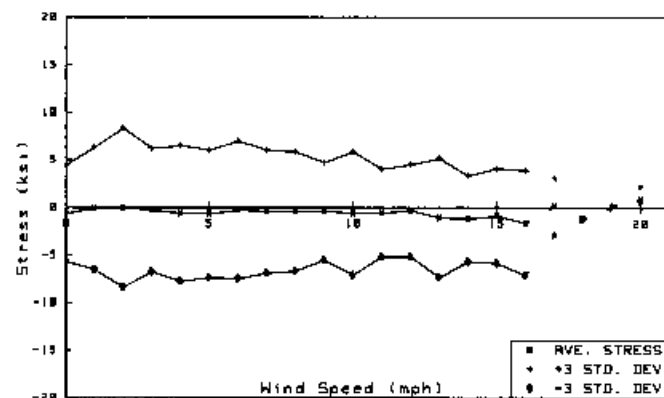


FIG. 5.—Stress Envelope for Midspan of 60-ft Structure

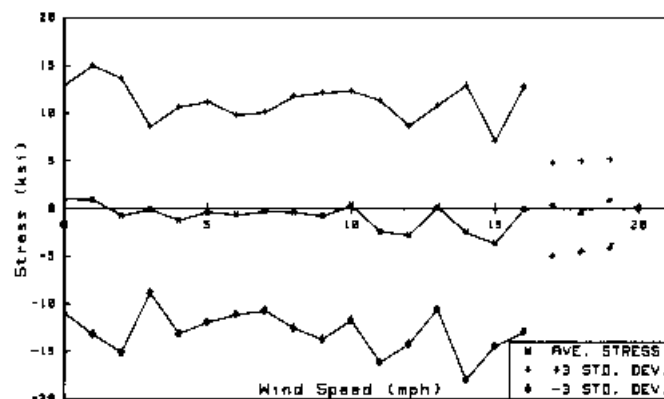


FIG. 6.—Stress Envelope for Midspan of 100-ft Structure

each nominal wind speed, the maximum positive and negative stresses were found, and the average stress and standard deviation were computed. The average positive and negative stresses along with their respective deviations were also determined.

The two locations of primary interest for each structure were the midspan of the beam and the base of the column. A stress envelope was determined for each of these by plotting the average stresses, along with points identifying values of ± 3 standard deviations to either side of the average. This envelope included 99.5% of all possible stress levels, assuming that the readings are normally distributed. The envelopes for the midspan of the 60-ft and 100-ft structures are shown in Figs. 5 and 6, respectively.

It can be seen that the maximum values of the stress envelopes are well within the safe range. For the 100-ft span structure, the maximum value given by the envelope is 18 ksi, which is only 53% of the yield stress of 34 ksi. For the 60-ft structure, the maximum value given by the

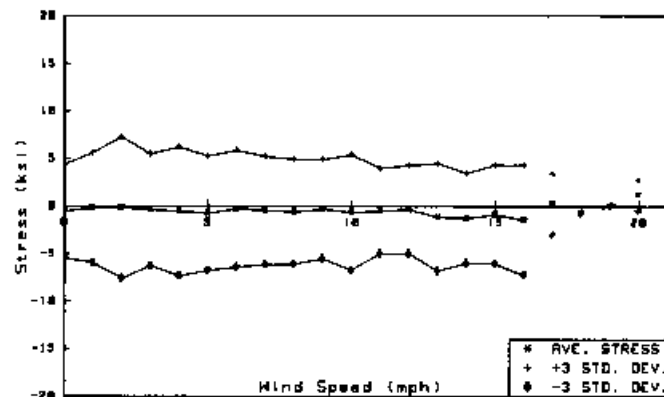


FIG. 7.—Stress Envelope for Column Base of 60-ft Structure

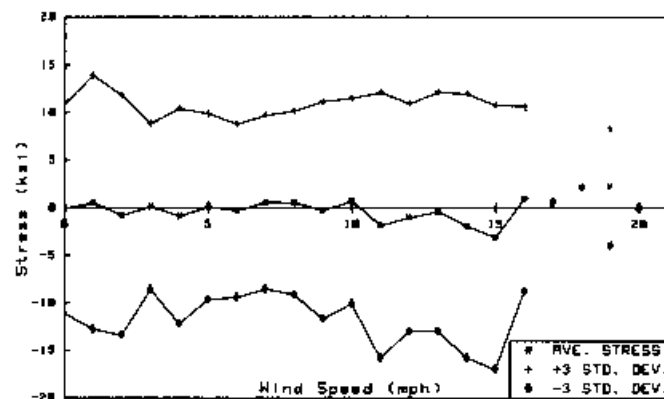


FIG. 8.—Stress Envelope for Column Base of 100-ft Structure

envelope is 8.2 ksi, or 24% of the yield stress. Furthermore, it is emphasized that these values are extremes. The large number of tests that were made lend confidence to the statistical evaluations: Further data are likely to alter neither the averages nor the ± 3 standard deviations to a significant degree. It is therefore clear that the low level of service load stress that was predicted by the analytical study has been substantiated.

It is interesting to note that both structures exhibit local maxima in the envelopes at wind speeds of approximately 2 mph, and again at 14–16 mph. The frequency of oscillations at 2 mph is well below any natural frequency for both structures. However, between wind speeds of 15 and 16 mph, both structures are near a natural frequency. For the 60-ft structure, the frequency corresponds to the third 3D mode of 3.26 cps. For the 100-ft structure, the mode is also the third 3D mode, at a frequency of 3.06 cps. It is believed that the maxima observed in the stress envelopes at this wind speed indicate that the structure is tending towards

resonance at these points. However, due to the structural damping and the gusting of the wind, the resonance condition is not achieved. This is the same finding that was made in the original monotube study (Ehsani, et al. 1985).

The bending stresses at the column bases are not as large as their midspan counterparts. The envelopes for the out-of-plane stresses for both structures are shown in Figs. 7 and 8. The maximum values are 7.7 ksi for the 60-ft structure and 17.0 ksi for the 100-ft structure. This demonstrates that the span length has a greater influence on the column base stresses than does the sign size. It is noted that the signs on the 60-ft structure were about twice as large as those on the 100-ft structure, but the latter has a span that is 67% longer. The column base stresses also exhibit local maxima at approximately the same wind speeds as were found for the beam.

The maximum stresses discussed so far were not the actual maximum stresses recorded, but the maximum values that are likely to occur given the statistical distribution of the data. The recorded stresses were less than those presented. For example, at 16 mph, the wind speed for which the stress envelope is the widest for the 60-ft structure, the maximum recorded stress was 7.3 ksi, as compared to the 8.2 ksi of the envelope. It is therefore clear that the use of a statistical approach has made it possible to include essentially all of the possible stress levels in the analysis. This also reflects the cyclic nature of the structural behavior, as well as the influence of the time lapse involved in the reading of the gages.

COMPARISON OF ANALYTICAL AND EXPERIMENTAL RESULTS

The full-scale test results that have been obtained represent an important addition to the pool of data that previously provided only theoretical results on the response of monotube sign support structures. In the following, a detailed evaluation of the data will be given, affording comparisons between actual in-service behavior of the structures and the

TABLE 2.—Computed and Measured Stress for 60-ft and 100-ft Structures

Wind speed (mph) (1)	In-Plane Stress ^a		Out-of-Plane Stress ^b		In-Plane Stress ^a		Out-of-Plane Stress ^b	
	Computed, ksi (2)	Measured, ksi (3)	Computed, ksi (4)	Measured, ksi (5)	Computed, ksi (6)	Measured, ksi (7)	Computed, ksi (8)	Measured, ksi (9)
2.5	4.38	5.52	1.34	1.74	10.11	9.74	2.84	3.25
5.0	4.38	5.69	1.34	2.08	10.18	9.96	2.87	5.39
7.5	4.39	4.33	1.35	1.08	10.23	9.96	2.91	4.98
10.0	4.39	4.86	1.48	2.03	10.29	9.91	2.95	4.13
12.5	4.49	4.36	1.65	1.73	10.51	9.60	3.11	4.04
15.0	4.54	4.10	1.61	2.43	10.70	9.13	3.16	5.36
17.5	4.59	4.01	1.70	2.58	10.53	4.33 ^c	3.12	1.47
20.0	4.66	1.30 ^d	1.81	1.65	10.75	— ^d	3.19	— ^d
22.1	—	—	—	—	10.92	— ^d	3.25	— ^d
22.5	4.71	— ^d	—	— ^d	—	—	—	—
23.2	5.11	— ^d	2.64	— ^d	—	—	—	—

^aAt midspan of beam.

^bAt base of column.

^cOnly one reading taken at this wind speed.

^dNo data collected for this wind speed.

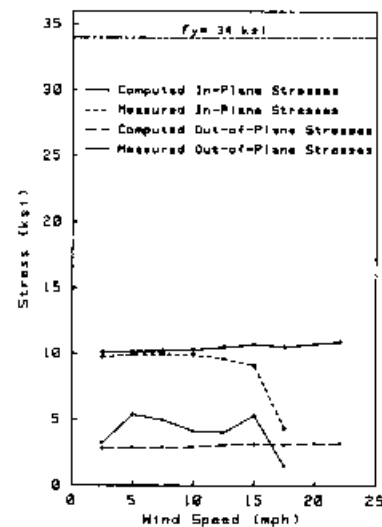
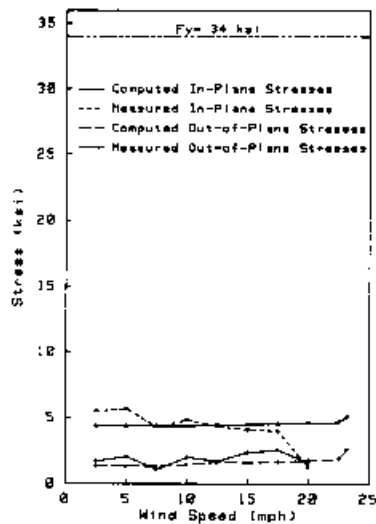


FIG. 9.—Correlation of Stresses for 60-ft Structure

FIG. 10.—Correlation of Stresses for 100-ft Structure

theoretical studies that have been made. In addition, the results will also be used to examine and verify the design recommendations that were made earlier (Ehsani, et al. 1985). It is noted that this earlier study examined the response of a variety of monotube structures, including the effects of high wind, sign placement, span, and stiffness of the structural components.

For the two structures, the analytical study and the field testing both showed the point of maximum in-plane stress to be at the midspan of the beam. The results are given in Table 2. It is interesting to note that for higher wind speeds, the in-plane stresses predicted in the analytical study were consistently higher than those measured in the field. Although the differences are generally acceptable, some discrepancies are to be expected due to modeling and loading assumptions.

In the out-of-plane direction, the point of maximum stress is the column base for both structures, and the results are shown in Table 2. It is seen that the analytical model predicts lower stresses than those that were measured. This is most likely due to the method used to model the beam-to-column connection.

Generally, good correlation was obtained between the analytical and experimental results. This is further shown in Figs. 9 and 10, which compare the computed and measured live load stresses for the two structures. It should be remembered that Figs. 9 and 10 show only live load stresses. It was not possible to measure the dead load stresses in the field, since both structures had been erected earlier. To obtain an indication of the total stress level, the dead load stresses from the analytical study were added to the measured live load stresses. These results are shown in Figs. 11 and 12. It can be seen that for both structures, the

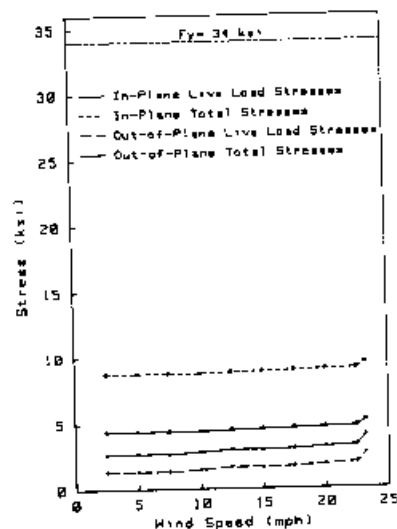


FIG. 11.—Total Stresses for 60-ft Structure

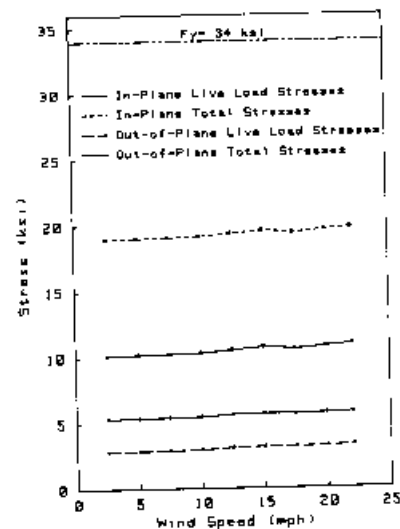


FIG. 12.—Total Stresses for 100-ft Structure

stresses are well below the yield stress of 34 ksi and the applicable allowable stress.

It should be noted that while the stresses for the structures are in the acceptable range, the deflections are well beyond the currently prescribed limits. This further indicates that the $d^2/400$ criterion is not suitable for monotube structures. If these had been designed to limit deflections to the $d^2/400$ limit, they would be overdesigned and probably uneconomical. A new deflection criterion, such as the one recommended by Ehsani, et al. (1985), needs to be adopted for use with monotube structures.

SUMMARY, CONCLUSIONS, AND RECOMMENDATIONS

The purpose of this study was to gather data on the performance of monotube sign support structures under service conditions. Through the use of field testing and computer modeling, data were collected to determine the service load response characteristics of the monotube structures.

On the basis of the two full-scale structures that have been tested and analyzed, the following conclusions can be made:

1. The service load stresses can be accurately predicted by the use of finite element modeling. The computer models in this study correlate very well with the field measurements, as well as with earlier analytical studies.
2. Due to the correlation between past and present results, the recommendations that have been made previously are well-founded and should be considered for adoption. These recommendations include

suggested methods of analysis, new performance criteria, and topics in need of further study.

3. The stress levels associated with the actual deflections are well below the magnitudes of the allowable stresses, even though the structures do not meet the $d^2/400$ deflection criterion.

4. The stress level at any point can be found by superimposing the stresses due to static loads and those due to dynamic loads.

5. The maximum in-plane stresses occur at midspan of the beam.

6. The maximum out-of-plane stresses occur at the column base.

7. Resonance did not occur in the field testing, even when vortices were shed at frequencies equal to the natural frequencies of the structures. This can be attributed to the inherent damping of the structure, as well as to the gusting nature of the wind.

8. Monotube structures of moderate to long spans (>60 ft) cannot meet the $d^2/400$ dead load deflection requirement of AASHTO. In most cases, it would prove to be very uneconomical to design such a structure to meet this requirement. It is recommended that the previously suggested deflection criterion should be adopted. This limits the dead load deflection-to-span ratio to a value of 1/150.

9. Since the maximum wind speeds were relatively low (23.2 mph), it is recommended that wind tunnel tests should be performed to evaluate the behavior of the structures under high wind conditions.

ACKNOWLEDGMENTS

This study was part of a larger research project sponsored by the Arizona Department of Transportation (ADOT). The interest and support provided by Frank R. McCullagh, Mumtaz Sarsam, and James R. Pyne are very much appreciated.

APPENDIX I.—METRIC CONVERSION TABLE

The following is provided for the conversion of units from U.S. Customary to S.I. Units:

1 in.	= 25.4 mm
1 ft	= 304.8 mm
1 ksi	= 6.89 MPa
1 mph	= 1.609 kmh

APPENDIX II.—REFERENCES

- American Association of State Highway and Transportation Officials (AASHTO). (1975). *Standard specifications for structural supports for highway signs, luminaires and traffic signals*. AASHTO, Washington, D.C. (revised 1978 and 1979).
- Ehsani, M. R., and Bjorhovde, R. (1986). "Deflection criteria for sign support structures." *J. Struct. Engrg.*, ASCE, 112(10), 2332-2341.
- Ehsani, M. R., Chakrabarti, S. K., and Bjorhovde, R. (1985). "Static and dynamic behavior of monotube span-type sign structures." *Report No. FHWA/AZ/194, I and II*, Arizona Dept. of Transp., Phoenix, Ariz.
- Fung, Y. C. (1955). *An Introduction to Aeroelasticity*. Wiley, New York, N.Y.
- Hoerner, S. F. (1965). *Fluid dynamic drag*. Hoerner Fluid Mechanics, Brick Town N.J.

Martin, Kipp A., Ehsani, M. R., and Bjorhovde R. (1985). "Field testing of monotube sign support structures." *Report No. ATTI-85-5*, Arizona Dept. of Transp., Phoenix, Ariz.

Weaver, W. (1961). "Wind-induced vibrations in antenna members." *J. Engrg. Mech. Div.*, ASCE, 87(1), 141-165.

APPENDIX III.—NOTATION

The following symbols are used in this paper:

A_p	=	projected area;
C_L	=	force coefficient;
\bar{C}_L	=	root-mean-square value of C_L ;
D	=	diameter of a tube;
d	=	vertical dimension (depth) of traffic sign;
$F(t)$	=	time-dependent force;
R	=	Reynolds number;
S	=	Strouhal number;
t	=	time;
V	=	wind velocity;
ρ	=	density of air; and
Ω	=	frequency of vortex shedding.